The solution for $\bar{\sigma}$ is given by:

$$\bar{\sigma}(\delta,p)=\frac{\alpha F_0}{kc}\,(p^2+2p)^{1/2}/[(c_e/c)^2-1]p^2+2(c_e/c)^2p]$$
$$\times\left\{e^{-(c_e/c)\delta(p^2+2p)^{1/2}}-e^{-\delta p}\right\} \tag{17}$$

Inversion yields:

$$\sigma(\beta,\delta)=-\frac{\alpha F_0}{kc}\,\frac{H(\beta-\delta)e^{-\beta}}{[1-(c_e/c)^2]}\{I_0(\beta^2-\delta^2)^{1/2}$$
$$+\frac{2e^{a(\beta-\delta)}}{[1-(c_e/c)^2]}\int_0^{\beta-\delta}e^{-a\eta}I_0(\eta^2+2\eta\delta)^{1/2}\,d\eta\}$$
$$+\frac{\alpha F_0}{kc}\,\frac{H(\beta-\bar{\delta})e^{-(\beta-\delta)}}{[1-(c_e/c)^2]}\{I_0(\beta-\bar{\delta})$$
$$+\frac{2e^{a(\beta-\delta)}}{[1-(c_e/c)^2]}\int_0^{\beta-\delta}e^{-a\eta}I_0(\eta)\,d\eta\} \tag{18}$$

where

$$a=[1+(c_e/c)^2]/[1-(c_e/c)^2]$$

Discussion of Results

Equation (18) indicates that there are 2 stress waves propagating down from the surface $x=0$, as shown pictorially in Fig. 1. The first stress wave propagates with the speed c. At the surface of this wave front $x=ct$ (or $\beta=\delta$), the stress is given by:

$$\sigma(\beta,\beta)=\frac{-\alpha F_0}{kc}\,\frac{1}{[1-(c_e/c)^2]}\,e^{-\beta}$$

This stress wave decays in the same way as the thermal wave front, and has the same magnitude as the thermal wave except by the factor of $1/[1-(c_e/c)^2]$. A second stress wave with propagation speed c_e follows. This result is in contrast to the conventional Fourier model which predicts the propagation of only one stress wave which has a speed of c_e (e.g., see Refs. 6 and 7).

As can be expected, under ordinary conditions, $c_e<<c$. This 2-wave phenomenon will be significant only during a very short transient. The first wave, like the thermal wave, decays rapidly with time. It has been pointed out in Ref. 5 that the difference in the surface temperatures between the Fourier and non-Fourier model becomes less than 1 percent in about $t\sim 0(50\alpha/c^2)$. However, at very low temperature, or when the order of magnitudes of c_e and c are comparable, this finite heat propagation speed cannot be ignored. The relaxation heat conduction equation must be used.

References

[1] Boley, B.A., "The Analysis of Problems of Heat Conduction and Melting," *High Temperature Structures and Materials,* Pergamon Press, New York, 1964, pp. 260-315.

[2] Peshkov, V., "Second Sound in He II," *Journal of Physics,* USSR, Vol. 8, 1944, p. 381.

[3] Chester, M., "Second Sound in Solids," *The Physical Revue,* Vol. 131, No. 5, Sept. 1963, pp. 2013-2015.

[4] Hsu, Y. Y., "On the Size Range of Active Nucleation Cavities on a Heating Surface, "*Journal of Heat Transfer,* Transactions of the ASME, Vol. 84, No. 3, Aug. 1962, pp. 207-216.

[5] Maurer, M. J. and Thompson, H. A., "Non-Fourier Effects at High Heat Flux," *Journal of Heat Transfer,* Transactions of ASME, Series C, Vol. 15, May 1973, pp. 284-286.

[6] Danilovskaya, V. Y., "Temperature Stresses in an Elastic Semi-Space Due to a Sudden Heating of its Boundary," Vol. 14, May-June 1950, pp. 316-318.

[7] Danilovskaya, V. Y., "On a Boundary Problem of Thermoelasticity," Prikladnaia Matematika i Mekhanika, Vol. 16, May-June 1952, pp. 341-344.

Wall-Wake Velocity Profile for Compressible Nonadiabatic Flows

Chen-Chih Sun* and Morris E. Childs†
University of Washington, Seattle, Wash.

Nomenclature

a = a constant in the expression $\tau=\tau_w(1-\eta^a)$ (see Ref. 5)
A = $\{[(\gamma-1)/2]\ M_e^2/(T_w/T_e)\}^{1/2}$
A_1 = $(Pr_t)^{1/2}\ \{[(\gamma-1)/2]\ M_e^2/(T_w/T_e)\}^{1/2}$
B = $\{(1+[(\gamma-1)/2]\ M_e^2/(T_w/T_e)\}$-1
B_1 = $\{(1+(Pr_t)^{1/2}\ [(\gamma-1)/2]\ M_e^2/(T_w/T_e)\}$-1
C = a constant in law of the wall (usually 5.1)
C_f = skin friction coefficient $\tau_w/(1/2)\rho_e u_e^2$
C_1 = $5.1-0.614/ak+(1/k)\ln(\delta U_\tau/\nu_w)$
K = constant in mixing length (usually 0.4)
M = Mach number
P = pressure
Pr_t = turbulent Prandtl number
T = temperature
u = velocity in streamwise direction
u^* = $(u_e/A)\arcsin\{[(2A^2u/u_e)-B]/(B^2+4A^2)^{1/2}\}$
u^{**} = $(u_e/A_1)\arcsin\{[(2A_1^2u/u_e)-B_1]/(B_1^2+4A_1^2)^{1/2}\}$
u_τ = friction velocity $(\tau_w/\rho_w)^{1/2}$
U^* = $u^*+(u_e/A)\arcsin\{B/(B^2+4A^2)^{1/2}\}$
W = Coles universal wake function
y = coordinate normal to wall
γ = ratio of specific heat
δ = boundary-layer thickness
δ^* = displacement thickness
Δ = $\int_0^\delta \frac{(u_e^{**}-u^{**})}{u_\tau}\,dy$
θ = momentum thickness
η = y/δ
ν = kinematic viscosity
Π = coefficient of wake function
ρ = density
τ = shear stress

Subscripts

e = freestream conditions
0 = stagnation conditions
w = conditions at the wall

Introduction

THE wall-wake velocity profile has been used to represent turbulent boundary-layer profiles for both adiabatic and nonadiabatic flows and for flows with or without pressure gradients.[1-5] A least squares fit of a wall-wake velocity profile to an experimental velocity profile may be used to determine C_f and δ for the profile. An accurate representation of the mean velocity distribution in the turbulent boundary layer can be very useful in integral analyses of turbulent flow problems. In the analysis of flows in which strong interactions occur (as for example in shock wave boundary-layer interactions) and in which combined viscid-inviscid analyses are required, a profile which provides a good representation of both C_f and δ can be quite important. With most earlier versions of the wall-wake profile, the velocity

Received Sept. 25, 1975; revision received March 15, 1976. This work was supported by NASA Grant NGR-48-002-047, under administration of the Aerodynamics Branch, Ames Research Center.

Index categories: Boundary Layers and Convective Heat Transfer – Turbulent; Supersonic and Hypersonic Flow.

*Research Assistant Professor, Department of Mechanical Engineering. Member AIAA.

†Professor and Chairman, Department of Mechanical Engineering. Member AIAA.

gradient at the boundary-layer edge has a nonzero value. The values of δ for these profiles may, as a consequence, correspond to points in the flow where viscous effects are substantial, especially in very high-speed flows. The purpose of this Note is to suggest a form of the wall-wake profile which is applicable to flows with heat transfer, and for which $\partial u/\partial y = 0$ at $y = \delta$. The modified profile, which takes into account the effect of turbulent Prandtl number, has been found to provide a good representation of experimental data for a wide range of Mach numbers and heat transfer. The C_f values which are determined by a least squares fit of the profile to the data agree well with values which were measured by the floating element technique. In addition, the values of δ determined by the fit correspond more closely to the outer edge of the viscous flow region than those obtained with earlier versions of the wall-wake profile.

Velocity Profile

The difference between the profile to be discussed here and some of the earlier versions is in the law-of-the-wall component. Van Driest[6] developed a compressible law-of-the-wall under the assumption of a turbulent Prandtl number of unity and a constant shear stress near the wall. It may be written as

$$\frac{u^*}{u_\tau} + \frac{u_e}{u_\tau}\frac{1}{A}\arcsin\frac{B}{(B^2+4A^2)^{1/2}} = \frac{1}{K}\ln\frac{yu_\tau}{\nu_w} + C \qquad (1)$$

With the addition of a wake component, Eq. (1) becomes

$$\frac{u^*}{u_\tau} + \frac{u_e}{u_\tau}\frac{1}{A}\arcsin\frac{B}{(B^2+4A^2)^{1/2}} = \frac{1}{K}\ln\frac{yu_\tau}{\nu_w} + C + \frac{\Pi}{K}W\left(\frac{y}{\delta}\right) \qquad (2)$$

The left-hand side of this expression is the transformed velocity U^* which is used in Refs. 3 and 4.

The use of Eq. (1) in a wall-wake profile results in a nonzero value of the velocity gradient at the boundary-layer edge. If we assume, as in Ref. 5, that τ may be expressed as $\tau = \tau_w(1-\eta^a)$, and, if for $Pr_t \neq 1$ the temperature distribution may be written as $(T/T_w) = 1 + B_1(u/u_e) - A_1^2(u/u_e)^2$ (see Ref. 7), with $(\rho/\rho_w) = 1/(T/T_w)$, we may follow the procedure used in Ref. 5 to obtain a wall-wake boundary-layer velocity profile of the following form:

$$\frac{u_e^{**}}{u_\tau} + \frac{u_e}{u_\tau}\frac{1}{A}\arcsin\frac{B_1}{(B_1^2+4A_1^2)^{1/2}} = \frac{1}{K}\{\ln\eta + \frac{2}{a}(1-\eta^a)^{1/2} - \frac{2}{a}\ln[1+(1-\eta^a)^{1/2}]\} + C_1\frac{\Pi}{K}W(\eta) \qquad (3)$$

For $a \to \infty$, which corresponds to the assumption of a constant shear stress distribution in the derivation of the compressible law-of-the-wall, and for $Pr_t \to 1$, $u^{**} \to u^*$, as in Eq. (2). Setting $\eta = 1$ in Eq. (3) yields the following expression for Π/K:

$$\frac{\Pi}{K} = \frac{1}{2}\left\{\frac{u_e^{**}}{u_\tau} + \frac{u_e^{**}}{u_\tau}\frac{u_e}{u_e^{**}}\frac{1}{A_1}\arcsin\frac{B_1}{(B_1^2+4A_1^2)^{1/2}} - \frac{1}{K}\ln\frac{\delta u_\tau}{\nu_w} - 5.1 + \frac{0.614}{aK}\right\} \qquad (4)$$

For mathematical convenience[1-3] we may replace $W(\eta)$ in Eq. (3) by $[1-\cos\eta\pi]$ and write the wall-wake velocity profile as

$$\frac{u}{u_e} = \frac{(B_1^2+4A_1^2)^{1/2}}{2A_1^2}\sin\left\{\left[\arcsin\frac{2A_1^2-B_1}{(B_1^2+4A_1^2)^{1/2}}\right] \times \left(1 + \frac{1}{K}\frac{u_\tau}{u_e^{**}}\left\{\ln\eta + \frac{2}{a}(1-\eta^a)^{1/2} - \frac{2}{a}\ln[1+(1-\eta^a)^{1/2}] - \frac{\Pi}{K}\frac{u_\tau}{u_e^{**}}(1+\cos\eta\pi)\right]\right\} + \frac{B_1}{2A_1^2} \qquad (5)$$

Results

The method of least squares has been used to fit the wall-wake profile, Eq. (5), to experimental velocity profiles reported by Hopkins and Keener,[8] Voisinet and Lee,[9] Horstman and Owen,[10] and Kilburg[11] for zero pressure gradient flows with heat transfer. The wall-wake velocities were obtained under the assumption of $Pr_t = 0.8$ and $a = 1$, the latter corresponding to the assumption of a linear shear stress distribution in the derivation of the law-of-the-wall. K was taken as 0.4 and C as 5.1. Data in the sublayer were excluded. The results shown here are from studies for which directly measured values of wall shear stress were reported.[8-10] The data reported in Refs. 8 and 9 were obtained on wind-tunnel walls. The data of Ref. 10 are for flow along the cylindrical surface of a cone-cylinder model whose axis was aligned with the primary wind-tunnel flow direction.

Comparisons of the experimental and wall-wake profiles are given in Fig. 1. Also shown on the figures are values of δ^*, θ, C_f, and Π/K as determined with the wall-wake profile. Experimental values of δ^*, θ, and C_f as obtained from the references also are listed. The wall-wake profile is seen to provide a good representation of the experimental velocity profiles. In addition, the C_f values determined by the fit of the proposed profile agree reasonably well with the directly measured values. For the data of Refs. 8 and 10, the values of δ determined by the fit correspond to points in the flow at which u/u_e, P_0/P_{0_e}, and T_0/T_{0_e} are essentially unity. If a is set equal to ∞ in Eq. (5), the values of ∞ are on the order of 5% lower than for $a = 1$ and the values of u/u_e, P_0/P_{0_e}, and ∞ are correspondingly lower. For reasons, which are not known at this time, the value of δ determined for the data of Ref. 9 corresponds to a point in the flow at which $u/u_e = 0.965$, $P_0/P_{0_e} = 0.56$, and $T_0/T_{0_e} = 0.938$, even though the wall-wake profile and the data agree very closely between the wall and the value of δ determined by the least squares fit. The authors comment on the temperature and history effects in some of their profiles. The rather low value of δ may be associated with these effects. For $a \to \infty$, δ is about 5% lower than for $a = 1$.

The wall-wake values of δ^* and θ agree well with experimental values for the data of Ref. 10. The larger differences for δ^* and θ for the data of Ref. 8 are because of differences between the temperature distribution for the experimental profile and the distribution for the wall-wake profile with $Pr_t = 0.8$. In the case of the profile from Ref. 9, the larger differences appear to result from the fact that the velocity, total temperature, and total pressure continue to increase well beyond the value of δ determined by the least squares fit.

The values of Π/K shown in Fig. 1 were determined from Eq. (4), assuming $Pr_t = 0.8$ and $a = 1$ and with u_τ and δ determined from the wall-wake fit. Note that the expression for ΠK differs from that used in Refs. 2-4 by virtue of the inclusion of the Prandtl number effect, through the term $0.614/aK$, and by virture of the differences in u_τ and δ which are obtained with the modified profile. Although the pressure gradient was zero for the three profiles shown, the values of Π/K are quite

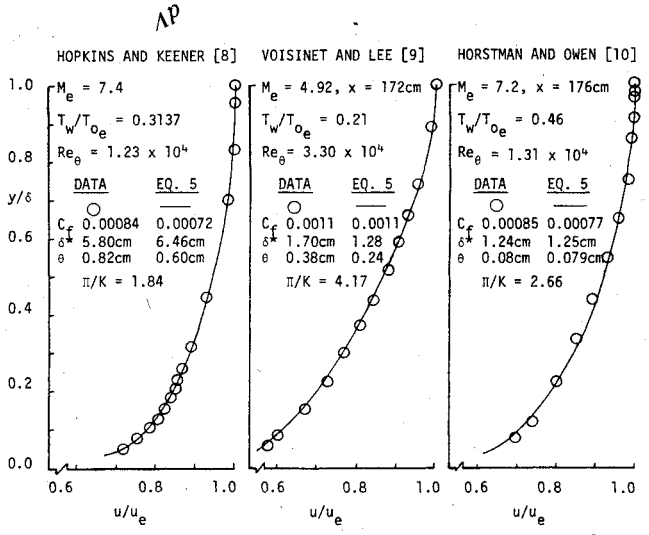

Fig.1 Velocity distributions in boundary layer with heat transfer.

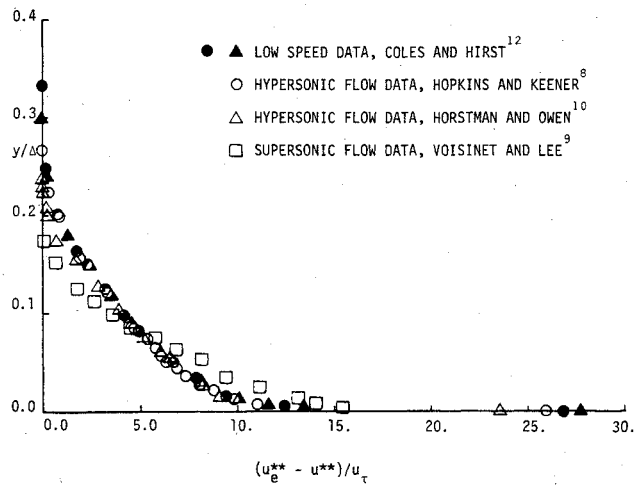

Fig.2 Comparison of generalized velocity defect for low-speed flow and compressible flow with heat transfer.

different. The values varied considerably from profile to profile for all of the data examined and generally tended to be higher than for low-speed or compressible adiabatic flows.

The experimental profiles also may be plotted in the form $(u_e^{**}-u^{**})/u_\tau$ vs y/Δ, where Δ is analogous to the defect thickness used by Gran et al.,[4] in their comparison of cold-wall, high-speed data with low-speed data[12]. Such a plot is shown in Fig.2. Although the profile from Ref.9 deviates from the low-speed results, the profiles from Refs. 8 and 10 correspond quite closely with the low-speed data. This suggests that the latter two profiles were nearer equilibrium than the former, which, in turn, may account for the fact that the value of δ determined for the profile from Ref. 9 does not correspond as closely to the viscid-inviscid flow boundary as was found for the other two profiles.

References

[1]Coles, D., "The Law of the Wake in the Turbulent Boundary Layer", *Journal of Fluid Mechanics,* Vol. 1, Pt. 2, 1956, pp. 191-226.

[2]Mathews, D.C., Childs, M.E., and Paynter, G.C., "Use of Coles' Universal Wake Function for Compressible Turbulent-Boundary Layers," *Journal of Aircraft*, Vol. 7, March-April 1970, pp. 137-140.

[3]Lewis, J.E., Gran, R.L., and Kubota, T., "An Experiment on the Adiabatic Compressible Turbulent Boundary Layer in Adverse and Favorable Pressure Gradients," *Journal of Fluid Mechanics,* Vol. 51, Pt. 4, 1972, pp. 657-672.

[4]Gran, R.L., Lewis, J.E., and Kubota, T., "The Effect of Wall Cooling on a Compressible Turbulent Boundary Layer," *Journal of Fluid Mechanics,* Vol. 66, Pt. 3, 1974, pp. 507-528.

[5]Sun, C.C. and Childs, M.E., "A Modified Wall-Wake Velocity Profile for Turbulent Compressible Boundary Layers," *Journal of Aircraft,* Vol. 10, June 1973, pp. 381-383

[6]Van Driest, E.R., "Turbulent Boundary Layer in Compressible Fluids," *Journal of the Aeronautical Sciences,* Vol. 18, 1951, pp. 145-160 and 216.

[7]Schlichting, H., *Boundary Layer Theory,* 6th ed., McGraw-Hill, New York, 1968, p. 669.

[8]Hopkins, E.J. and Keener, E.R., "Pressure-Gradient Effects on Hypersonic Turbulent Skin Friction and Boundary-Layer Profiles," *AIAA Paper,* No. 72-215., June 17-19, 1972.

[9]Voisinet, R.L.P. and Lee, R.E., "Measurement of a Mach 4.9 Zero Pressure-Gradient Turbulent Boundary Layer with Heat Transfer, Part I--Data compilation," *NOLTR* 72-232, Sept. 1972, Naval Ordnance Laboratory, White Oak, Silver Spring, Md.

[10]Horstman,C. and Owen, F., "Turbulent Properties of a Compressible Boundary Layer,"*AIAA Journal,*Vol. 10, Nov. 1972, pp. 1418-1424.

[11]Kilburg, R.F., "Experimental Investigation of the Interaction of a Plane, Oblique, Incident-Reflection Shock Wave with a Turbulent Boundary Layer, on a Cooled Surface," CR-66841-3, Oct. 1969, NASA.

[12]Coles, D.E., and Hirst, E.A., "Computation of Turbulent Boundary Layers," *Proceedings of AirForce Office of Scientific Rysearch-Standard Conference,* Vol. 2, AFOSR-2FP, 1968, Stanford University, Calif.

General Thermal Constriction Parameter for Annular Contacts on Circular Flux Tubes

M. Michael Yovanovich*
University of Waterloo, Waterloo, Ontario, Canada

Introduction

In a recent paper,[1] a general expression was obtained for constriction resistances due to arbitrary flux distributions over circular contact areas on a circular flux tube. By means of the general expression, special cases such as the isothermal and constant flux boundary condition could be evaluated. This paper extends that mathematical development to the more general case of an annular contact area supplying heat to a coaxial circular flux tube.

Problem Statement and Solution

An annular contact area of radii a, b ($a < b$) is situated on the end of a solid circular cylinder of radius c (Fig. 1). The long cylinder, whose thermal conductivity is k, is perfectly insulated except for the annular contact area where the flux is prescribed. For the analysis to follow, a circular cylinder coordinate system (r, z) is chosen, and the origin is placed on the axis of the cylinder.

Since there is steady heat flow through the cylinder, the governing equation is

$$\frac{\partial^2 T}{\partial r^2} + \frac{1}{r}\frac{\partial T}{\partial r} + \frac{\partial^2 T}{\partial z^2} = 0 \tag{1}$$

and the boundary conditions are

$$z=0, \quad 0\le r<a, \quad \partial T/\partial z = 0 \tag{2a}$$

$$a<r<b, \quad -k(\partial T/\partial z) = f(r) \tag{2b}$$

$$b<r\le c, \quad \partial T/\partial z = 0 \tag{2c}$$

Received Jan. 26, 1976, revision received March 8, 1976.

Index categories: Spacecraft Temperature Control Systems; Heat Conduction; Thermal Modeling and Experimental Thermal Simulation.

*Visiting Professor, Department of Mechanical Engineering, Massachusetts Institute of Technology, Cambridge, Mass. Associate Fellow AIAA.